Journal of Sound and Vibration 392 (2017) 382–399

Contents lists available at ScienceDirect

Journal of Sound and Vibration

journal homepage: www.elsevier.com/locate/jsvi

From phase drift to synchronisation – pedestrian stepping behaviour on laterally oscillating structures and consequences for dynamic stability

Mateusz Bocian [a,*], Jeremy F. Burn [b], John H.G. Macdonald [c], James M.W. Brownjohn [d]

[a] Department of Engineering, University of Leicester, University Road, Leicester LE1 7RH, UK
[b] Department of Mechanical Engineering, University of Bristol, University Walk, Bristol BS8 1TR, UK
[c] Department of Civil Engineering, University of Bristol, University Walk, Bristol BS8 1TR, UK
[d] Vibration Engineering Section, University of Exeter, North Park Road, Exeter EX4 4QF, UK

ARTICLE INFO

Article history:
Received 6 April 2016
Received in revised form
26 November 2016
Accepted 13 December 2016
Available online 22 December 2016

Keywords:
Human-structure interaction
Synchronous lateral excitation
Self-excited forces
Instrumented treadmill
Human loading
Structural stability

ABSTRACT

The subject of this paper pertains to the contentious issue of synchronisation of walking pedestrians to lateral structural motion, which is the mechanism most commonly purported to cause lateral dynamic instability. Tests have been conducted on a custom-built experimental setup consisting of an instrumented treadmill laterally driven by a hydraulic shaking table. The experimental setup can accommodate adaptive pedestrian behaviour via a bespoke speed feedback control mechanism that allows automatic adjustment of the treadmill belt speed to that of the walker. 15 people participated in a total of 137 walking tests during which the treadmill underwent lateral sinusoidal motion. The amplitude of this motion was set from 5 to 15 mm and the frequency was set from 0.54 to 1.1 Hz. A variety of stepping behaviours are identified in the kinematic data obtained using a motion capture system. The most common behaviour is for the timing of footsteps to be essentially unaffected by the structural motion, but a few instances of synchronisation are found. A plausible mechanism comprising an intermediate state between unsynchronised and synchronised pedestrian and structural motion is observed. This mechanism, characterised by a weak form of modulation of the timing of footsteps, could possibly explain the under-estimation of negative damping coefficients in models and laboratory trials compared with previously reported site measurements. The results from tests conducted on the setup for which synchronisation is identified are evaluated in the context of structural stability and related to the predictions of the inverted pendulum model, providing insight into fundamental relations governing pedestrian behaviour on laterally oscillating structures.

1. Introduction

It is now well known that walking pedestrians have a capacity to cause lateral dynamic instability of structures [1]. Whether divergent-amplitude lateral structural vibrations will develop under the action of walking pedestrians depends on

* Corresponding author.
E-mail address: m.bocian@leicester.ac.uk (M. Bocian).

http://dx.doi.org/10.1016/j.jsv.2016.12.022
0022-460X/

the net damping of the crowd-structure system. The initiation of dynamic instability for a given vibration mode will occur when the total negative damping of the mode from the pedestrians is greater in magnitude than the structural damping. The most widely publicised occurrence of pedestrian-induced instability is the case of the London Millennium Footbridge which suffered from excessive vibrations on the day of its opening. Subsequently, a series of controlled crowd loading tests was conducted on that bridge of which results showed that pedestrian lateral force is approximately proportional to the lateral velocity of the deck. It was proposed to model this force as a damping coefficient per pedestrian, having an empirical numerical value of –300 N s m^{-1} for structural vibration modes within the frequency range 0.5–1 Hz [2]. This modelling framework was later extended to account for the component of pedestrian lateral force at the frequency of the excited vibration mode orthogonal to the one in phase with structural velocity [3]. Similar to the approach adopted in wind engineering for modelling flutter [4], after appropriate scaling, the components in phase with velocity and acceleration can be expressed as equivalent added damping and mass to the structure [e.g. 5–7], denoted herein as ΔC and ΔM, respectively, and expressed per pedestrian. This framework implies that ΔC and ΔM, which are often termed as self-excited (or motion-dependent) forces, are in fact independent of bridge motion amplitude, which might not always be the case. Nevertheless, it has become a convention to express self-excited pedestrian forces in this concise form. The effect of ΔM is effectively to change the vibration frequency, which should be accounted for in analyses of dynamic structural stability as, at least in theory, this could in turn have an effect of modifying ΔC [7]. ΔC itself is more important as it can become negative hence effectively reduce the total damping. However, what value of ΔC should be used for the assessment of structural stability remains an open issue. This is because a discrepancy exists between the measurements of ΔC obtained from tests on full-scale structures, representing a top-down approach to the derivation of self-excited forces, and results of laboratory investigations on the behaviour of a single walker, representing a bottom-up approach.

The values obtained using a top-down approach, relying on back-calculation of ΔC from the measured structural response, are summarised in Table 1.

It can be seen that, with the exception of ΔC derived from the behaviour of the Clifton Suspension Bridge, all the values fall at or below –300 N s m^{-1}. This is considerably lower than the average values reported from an extensive experimental campaign of Ingólfsson et al. [5], which reached a minimum of approximately –200 N s m^{-1} for a vibration amplitude of 4.5 mm, but increased to above half that value (hence became less detrimental in the context of structural stability) for vibration amplitudes above 20 mm. This seems inconsistent with the measurements on the London Millennium Footbridge, for which ΔC was found to be fairly constant up to the maximum vibration amplitude of 48 mm experienced in the tests [2]. The recent laboratory results reported by Bocian et al. [11] concur in that respect, suggesting that the expected ΔC for a mode at 0.9 Hz vibrating with an amplitude of 10 mm would be just –150 N s m^{-1}, accounting only for pedestrians unsynchronised to the lateral motion, walking at their preferred unimpeded speed.

It is noteworthy that during the tests on instrumented treadmills aiming at quantification of self-excited forces the speed of the walker was either imposed (equal to the preferred walking speed on an unactuated treadmill) [2], or self-selected (i.e. unconstrained) due to the application of a treadmill belt speed feedback control mechanism [11]. All these speeds might not correspond to the speed of a pedestrian walking in a dense crowd, which can be expected to reduce with increasing crowd density. The predictions of the inverted pendulum pedestrian model (IPM) proposed by Macdonald [6] suggest that ΔC can then become more detrimental, for the range of natural frequencies coinciding with the frequencies of the excited modes listed in Table 1 [7]. This might explain the large negative values of $^{.5823mm,lt)=\text{"}graphic:mml:print:m440856860_2 8010\text{"}}$ observed on most of the bridges identified in Table 1 [12]. However experimental evidence is currently lacking to validate this prediction.

Another suggested explanation of the discrepancy in ΔC derived using bottom-up and top-down approach is preferential phase frequency entrainment [13]. This is a state in which the pedestrians synchronise their motion to the motion of the vibrating structure, adjusting their relative phase such as to input more energy into the excited structural mode than the average expected ΔC for unsynchronised walking. It has been suggested that this behaviour might be driven by a desire to avoid less comfortable gait patterns in which the step width becomes narrow or the position of the foot during a step crosses to the contralateral side of the body [14]. However, no experimental evidence has been presented supporting the prevalence of preferential phase frequency entrainment or even its very existence.

To address the uncertainty as to the discrepancy between self-excited forces obtained using top-down and bottom-up approaches, the aim of this study is to evaluate temporal pedestrian stepping behaviour on laterally oscillating structures and its consequences for structural stability. To this end a series of tests was performed on a laterally oscillating instrumented treadmill in which kinematic data of the behaviour of walkers were collected with a motion capture system. Critical for realising the aim of this study is the capacity of the experimental setup to accommodate adaptive pedestrian behaviour via a bespoke speed feedback control mechanism that allows automatic adjustment of the treadmill belt speed to

Table 1
Pedestrian damping coefficient identified from tests on full scale structures. The values in brackets denote the natural frequencies of the relevant modes.

	London Millennium Footbridge [2]	**Changi Mezzanine Bridge** [8]	**Clifton Suspension Bridge** [9]	**Pedro and Inês Footbridge** [10]
ΔC [N s m^{-1}]	–300 (0.5 & 1 Hz)	–376 (0.9 Hz)	–160 (0.52 Hz) & –210 (0.74 Hz)	–300 (0.91 Hz)

that of the walker. After this introduction, Section 2 briefly presents the experimental setup, the protocols applied during the tests and data processing methods. Five different types of stepping behaviour identified from the collected data are described in Section 3. These include phase drift, phase pulling, intermittent frequency entrainment, frequency locking and non-uniform distribution of phase angles. Since phase drift has already been described in detail in [11], the focus in the current study in on the phase pulling and synchronisation mechanisms. Phase pulling occurs when the duration of pedestrian steps changes systematically depending on the timing of footsteps relative to lateral structural motion. This behaviour, which has never been observed before in experimental data, is shown to be able to explain the aforementioned discrepancy between the self-excited forces. The possibility of the occurrence and the consequences of synchronisation on structural stability are considered in Section 4 in which the experimental results, quantified in terms of self-excited forces, are also related to the predictions of the IPM, providing a template of pedestrian behaviour on laterally oscillating structures. Overall conclusions are stated in Section 5.

2. Materials and methods

2.1. Equipment

A novel experimental setup developed at the University of Bristol was used in this study. In short, the setup consists of:

- an instrumented treadmill supported on a hydraulic motion base, providing a 1.5 m wide and 2 m long laterally actuated walking platform;
- a treadmill speed feedback control mechanism that allows automatic adjustment of the treadmill belt speed to that of the walker;
- a motion capture system consisting of six infrared cameras (Oqus 3, Qualisys), used to collect kinematic data;
- an immersive virtual reality environment provided via nVisor SX111 stereoscopic head-mounted display.

Full details on this setup and its validation are available in [11] and [15]. Fig. 1 shows a subject during a test on the experimental setup. The insertion in Fig. 1 shows an example of the computer generated image projected onto the left-eye screen of the head-mounted display.

2.2. Participants

Twelve males and three females volunteered in the tests. The means and standard deviations of the basic parameters for the whole cohort are, respectively: 23.8 and 4.8 years for age, 75.9 and 14.3 kg for mass and 1.82 and 0.08 m for height. All subjects were adults, naïve as to the purpose of the experiments and without any known conditions which could impair their performance. All subjects had experience with walking on a treadmill prior to participating in the study. All subjects signed an informed consent form before commencing the experiments. The study was approved by the University of Bristol Ethics of Research Committee.

2.3. Procedures

Each subject conducted several tests during which the treadmill underwent a sinusoidal lateral motion. The amplitude of

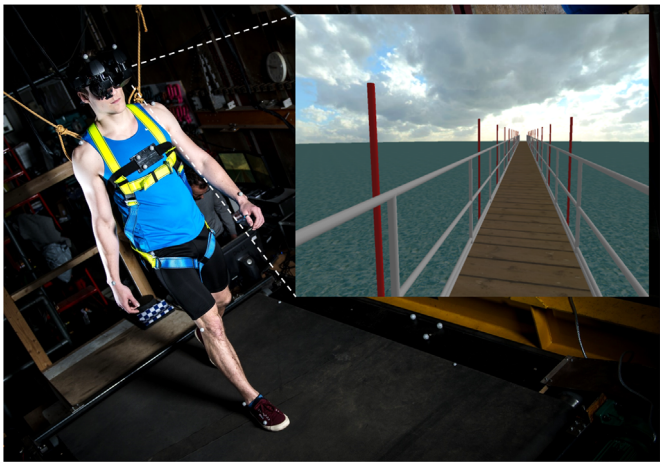

Fig. 1. A subject during a test on the custom-built instrumented treadmill.

this motion was set to 5 mm, 10 mm or 15 mm, and the frequency was set to 0.54 Hz, 0.76 Hz, 0.9 Hz or 1.1 Hz. 137 tests were conducted in total on the laterally oscillating treadmill, each lasting between 2 to 3 minutes which, after discarding periods of gait and setup initiation and termination stages, gave approximately 1 to 2 minutes of data for further processing. Before any recordings were made, each subject was given approximately 10 minutes to habituate to the experience of walking on the treadmill in different combinations of base motion and visual conditions applied during the tests. The visual environment varied from that of the lab to different scenarios applied with virtual reality, consisting of a bridge and different surroundings (see example in Fig. 1). Different visual environments were applied for a different research purpose, but the data enabled different types of temporal stepping behaviours adopted by pedestrians in response to laterally oscillating walking surface to be identified. Since the same types of stepping behaviours were found for all visual environments applied during the tests, visual conditions are not treated in the analyses as an independent variable.

2.4. Data processing

All data collected during tests were sampled at 128 Hz.

The dynamics of the pedestrian-structure system are analysed according to a mathematical convention [16], by constructing a discrete map of instantaneous phase between the pedestrian and structural motion at a suitable point in the gait (or step) cycle. For gait analysis, a convenient event for the construction of this map is the instant of touchdown of a foot to the walking surface, which marks the beginning of each step. This event is associated with an abrupt change in foot motion, which is relatively easily identifiable from kinetic and kinematic gait data.

The instance of touchdown, marking the beginning of a step and the double-support phase of gait, was identified from vertical velocity signals of the motion capture system marker placed on the lateral malleolus, using the method of O'Connor et al. [17]. The instance of take-off, i.e. the time when the foot loses contact with the walking surface, marking the end of step and double-support phase of gait, was identified from the fore-aft velocity of the motion capture system marker placed on the fourth metatarsal, using the method of Ghoussayni et al. [18].

The beginning of the treadmill lateral vibration cycle was taken when the treadmill displacement was zero and its velocity was towards the right of the walker. Pedestrian stepping behaviour was quantified by means of the phase angle between the pedestrian and bridge motion, ψ, at the instant of the heel strike (the terms *heel strike* and *touchdown* are used interchangeably herein), t_{TD}, in relation to the treadmill vibration period (equal to reciprocal of vibration frequency f_b):

$$\psi = 2\pi\left(t_{TD} - t_{b,0}\right)f_b \tag{1}$$

where $t_{b,0}$ is the time of the most recent beginning of a treadmill vibration cycle. This is visualised in Fig. 2.

It is noteworthy that the symmetry in pedestrian behaviour associated with the bipedal nature of human gait implies that compatible phase angles for the right and the left legs are shifted relatively by π. For example, a phase angle of 0.5π measured for the right leg touchdown, occurring when the treadmill is at the rightmost position relative to the direction of progression of the walker corresponds with a phase angle of 1.5π measured for the left leg touchdown, occurring when the treadmill is at the leftmost position relative to the direction of progression. Therefore, the set of phase angles in which data for the left leg are shifted by π and, if necessary, wrapped to be within the range 0 to 2π is hereafter called the set of compatible phase angles, denoted by the symbol ψ_c.

Pedestrian-induced self-excited forces at the treadmill oscillation frequency were quantified in terms of the equivalent added damping and mass to the structure (ΔC and ΔM, respectively). In the calculation of the self-excited forces the length of the data record was taken containing, as closely as possible, an integer number of pedestrian and bridge vibration cycles, making provision for the type of evolution of phase angle. This ensured the obtained ΔC and ΔM were representative of the average pedestrian behaviour during any given test. It also allowed the calculation of the self-excited forces to be simplified to the following two equations [11]:

$$\Delta M = -\mathrm{Re}\left[H_{\ddot{x}_b F}(f_b) - \widehat{H}_{\ddot{x}_b F}(f_b)\right] \tag{2}$$

$$\Delta C = \mathrm{Im}\left[H_{\ddot{x}_b F}(f_b) - \widehat{H}_{\ddot{x}_b F}(f_b)\right]\omega_b \tag{3}$$

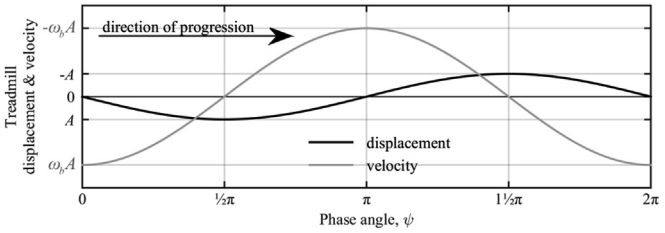

Fig. 2. Adopted convention for the definition of phase angle ψ of the instant of the touchdown relative to the most recent beginning of a treadmill vibration cycle. A and $\omega_b = 2\pi f_b$ denote the treadmill displacement amplitude and angular vibration frequency, respectively.

where Re[•] and Im[•] denote the real and imaginary part of the complex number •, respectively, ω_b is the angular oscillation frequency of the treadmill and $H_{\ddot{x}_b F}(f_b)$ and $\widehat{H}_{\ddot{x}_b F}(f_b)$ are the transfer functions between the measured treadmill acceleration and lateral force, evaluated at the oscillation frequency. $H_{\ddot{x}_b F}(f_b)$ and $\widehat{H}_{\ddot{x}_b F}(f_b)$ were found from the ratio of Fast Fourier Transforms of the force and acceleration signals, the difference being that the former was obtained from data collected in the presence of the walking pedestrian while the latter was obtained for the empty treadmill with the belt set to run at a constant speed to account for the inertia forces and possible dynamics of the treadmill itself.

The Lomb-Scargle algorithm was used to obtain power spectra of unevenly spaced data [19], to uncover the components of variability of time between hell strikes serving in the identification of the type of pedestrian stepping behaviour. The advantage of this method is that it does not require interpolation, which can often introduce spurious power at low frequencies, and allows the significance of the identified components of the spectrum to be readily estimated [20]. Before obtaining the power spectrum, the algorithm requires normalisation of the data by subtraction of the mean.

3. Pedestrian stepping behaviour on laterally oscillating structure

Five types of pedestrian stepping behaviour on laterally oscillating structure were identified from the analysis of the measured phase angles and are presented in this section. These are: phase drift, phase pulling, intermittent frequency entrainment, persistent frequency locking and non-uniform distribution of phase angles. Of these, phase drift is mentioned only briefly since this behaviour has been already reported in detail in [11]. It needs to be pointed out that the terms ‘frequency locking’ and ‘frequency entrainment’ are sometimes used synonymously [16]. However, a distinction is made herein in that ‘frequency entrainment’ refers to synchronisation of the first order only, i.e. $f_p/f_b = 1$, with any phase difference, whereas ‘frequency locking’ is more general and refers to synchronisation of any order, i.e. $f_p/f_b = \{1, 2\}$, with any phase difference, where f_p is the average pedestrian stride frequency which is equal to half step frequency since one stride consists of two steps. A summary of the conducted tests with reference to the identified pedestrian stepping behaviour is presented in Table 2.

3.1. Phase drift

This was the most common type of pedestrian stepping behaviour (see Table 2). It is characterised by close to uniform distribution of phase angles, due to the stride frequency being fairly constant and different from the bridge vibration frequency. The phase angle evolves in this case at a nearly constant rate and the variation of time between heel strikes, analysed with the Lomb-Scargle algorithm, shows no significant components apart from the one at the average stride frequency [20]. An example of phase drift is shown in Fig. 3.

Successive steps on the right (•) and left (○) legs are joined by black lines. Four grey lines plotted at the beginning of the record, each underlying data points for one leg during one phase angle evolution cycle, are the best linear fits. It can be seen that the gradients of these lines are similar, indeed confirming that the phase evolves at a nearly constant rate.

3.2. Phase pulling

This type of behaviour is characterised by a non-uniform distribution of phase angles and orderly phase evolution. Five cases of phase pulling showing multiple cycles of evolution of the phase angle throughout its entire range were identified for four different subjects, for walking with four different treadmill vibratory conditions. The details of these tests are presented in Table 3. The results can be divided into two groups for which the average stride frequency was slightly higher

Table 2
Summary of the conducted tests.

Vibration amplitude A [mm]	Vibration frequency f_b [Hz]	Number of conducted tests	Phase drift	Phase pulling	Persistent frequency locking	Intermittent frequency entrainment	Non-uniform distribution of phase angles
5	0.54	14	10	0	0	0	4
5	0.76	18	12	1	0	0	5
5	0.9	13	8	1	0	2	2
5	1.1	13	9	0	0	0	4
10	0.54	12	9	0	1	0	2
10	0.76	11	10	0	0	0	1
10	0.9	44	31	2	1	4	6
10	1.1	6	4	1	0	0	1
15	0.54	2	1	0	0	0	1
15	0.76	2	1	0	0	0	1
15	0.9	2	1	0	0	1	0
Total		137	96	5	2	7	27

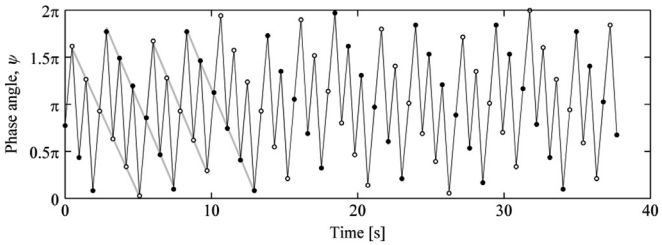

Fig. 3. Pedestrian behaviour and its consequences in the case of phase drift identified for f_b = 0.9Hz, A = 5mm, f_p = 1.09Hz. Phase angles for the right and left leg touchdowns are denoted by • and ○, respectively.

or lower than the treadmill lateral oscillation frequency. Examples of these types of behaviour are presented in Sections 3.2.1 and 3.2.2, respectively. It needs to be remarked that more cases of possible phase pulling were identified in which the evolution of the phase angle was either too slow to complete more than one full cycle or indicated that the walker changed their stepping behaviour during the test. These tests fall into the category 'non-uniform distribution of phase angles' in Table 2. Since the evidence of phase pulling in these cases is uncertain, they are omitted from further analysis. To better understand the significance of phase pulling and the flow of energy between the components of the pedestrian-structure system, the work done by the pedestrian on the treadmill is quantified in Section 3.2.3. The possibility of the occurrence of phase pulling is subsequently discussed in Section 3.2.4.

3.2.1. Phase pulling for the average stride frequency higher than the treadmill oscillation frequency

An example of phase pulling is presented in Fig. 4(a) for a test with f_b = 0.9Hz, A = 10mm, f_p = 0.94Hz, h = 1.81m and m_p = 75kg (see Table 3). The phase angles corresponding to the right and left leg touchdowns, denoted by • and ○ respectively, do not evolve in equal increments but vary non-linearly. To make this clear, best fit straight lines were fitted to the data in ranges in which the phase angles evolve distinguishably faster and slower and denoted in Fig. 4(a) by lines underlying data points. Faster evolution of phase angles in the range from π to 2π for the right leg, and in the range from 0 to π for the left leg, are in fact compatible since the corresponding phase angles for both legs are shifted exactly by π (see Section 2.4).

The distribution of phase angles and its consequences are presented in more detail in Fig. 4(b) to (d). The phase angles presented in Fig. 4(a) are plotted against time, which is consistent with the plot of the time between heel strikes, T_{TD}, presented in Fig. 4(b). The regions in Fig. 4(b) where the values of time between heel strikes fall consistently below the mean value, denoted by a dashed line, i.e. in time intervals 11 to 20 s, 40 to 48 s and 66 to 73 s, are representative of the regions in Fig. 4(a) where the patterns of phase angles have the steepest negative gradients. In those cases the subject walked with a stride frequency which was relatively higher (up to approximately 0.1 Hz) than the treadmill lateral vibration frequency. This can be seen by relating data points in Fig. 4(b) to the black line representing half of the bridge vibration period at $(2f_b)^{-1}$. Conversely, the values in Fig. 4(b) which lie at the top of the plot indicate stride periods in the vicinity of the treadmill lateral vibration period, i.e. time intervals 0 to 11 s, 20 to 40 s, 48 to 66 s and 73 to 75 s, hence regions where the phase angle evolves more slowly in Fig. 4(a).

Fig. 4(c) presents histograms of phase angles for the right and leg touchdowns with a bin size of π/16. The distributions of the phase angles for both legs are clearly non-uniform with the touchdowns of the right leg occurring predominantly with phase angles in the range from π/8 to 17π/16 and the touchdowns of the left leg occurring predominantly with phase angles in the range from 0 to π/16 and from 18π/16 to 31π/16. The ranges of densification of phase angles for both legs are in fact compatible.

Fig. 4(d) presents the normalised power spectrum of the time history of the time between heel strikes, from the data presented in Fig. 4(b), obtained using the Lomb-Scargle algorithm. It can be seen that there is a dominant sinusoidal component of the signal at a frequency of 0.037 Hz, which has a significance level greater than 0.999. This component, corresponding to the beating frequency between the treadmill lateral oscillation frequency and the average pedestrian

Table 3
Details of tests in which phase pulling was identified.

Gender	Height [m]	Mass m_p [kg]	Vibration amplitude [mm]	Vibration frequency [Hz]	Average stride frequency f_p [Hz]	Average treadmill velocity [ms^{-1}]	Normalised equivalent added damping $\Delta C/m_p$ [s^{-1}]	Normalised equivalent added mass $\Delta M/m_p$ [–]
male	1.84	85	5	0.76	0.72	0.8	−9.05	−1.39
male	1.76	56	5	0.9	0.87	1.1	−8.73	−0.13
male[a]	1.81	75	10	0.9	0.94	1.2	−0.35	0.11
male[a]	1.81	75	10	0.9	0.93	1.2	1.8	0.2
female	1.64	51	10	1.1	1.08	1.7	−0.53	0.33

[a] denotes the same subject.

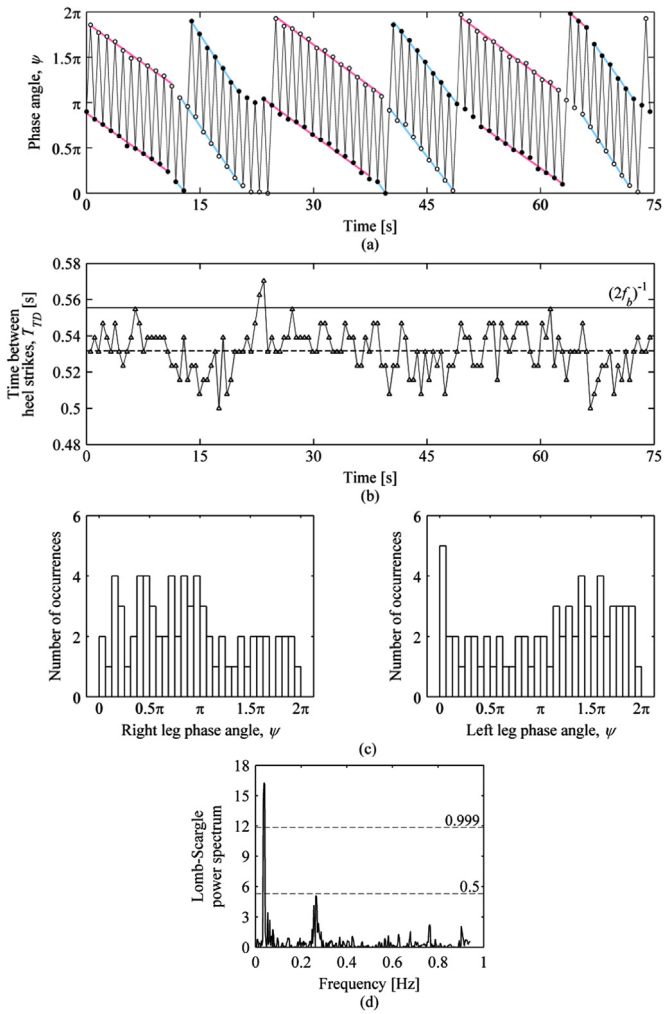

Fig. 4. Pedestrian behaviour and its consequences in the case of phase pulling identified for $f_b = 0.9$Hz, $A = 10$mm, $f_p = 0.94$Hz. (a) Phase angle for right (•) and left (○) leg touchdowns. (b) Time between heel strikes with dashed line representing the mean value and continuous line representing half of the treadmill vibration period. (c) Histograms of phase angles for leg touchdowns, with bin size of $\pi/16$. (d) Lomb-Scargle normalised power spectrum of time between heel strikes with significance levels denoted by dashed lines.

stride frequency and having a period of approximately 27 s, reveals itself in Fig. 4(b) in a wavelike pattern of the time between heel strikes with regions of low values occurring in regular intervals. Note another component of the spectrum clearly visible at a frequency of 0.266 Hz. This component does not exceed a significance level of 0.5 which marks an upper boundary for components which could be expected by chance [20].

3.2.2. *Phase pulling for the average stride frequency lower than the treadmill oscillation frequency*

A different example of phase pulling, based on data from a test during which $f_b = 0.9$Hz, $A = 5$mm, $f_p = 0.87$Hz, $h = 1.76$m and $m_p = 56$kg (see Table 3), is presented in Fig. 5. Unlike for the data in Fig. 4(a), the gradient of the evolution of the phase angle is here generally positive since $f_p < f_b$. However, similarly to those data, the rate of evolution of ψ changes in different ranges. This causes bias in the distribution of phase angle, as can be seen in Fig. 5(c). In this case, however, the most populated bins on the histograms are approximately shifted by π in comparison to those presented in Fig. 4(c) for which $f_p > f_b$. The only significant component of variation of time between heel strikes in Lomb-Scargle power spectrum presented in Fig. 5(d) is at a frequency of 0.033 Hz. Similarly to the case discussed in Section 3.2.1, this component corresponds to the beating frequency between the treadmill lateral oscillation frequency and the average pedestrian stride frequency, having a period of 30 s, approximately matching the oscillation of the signal in Fig. 5(b).

3.2.3. *Phase pulling and asymmetry in energy flow between components of pedestrian-structure system*

To better understand significance of phase pulling it is worth to look at the data from the point of view of energy flow

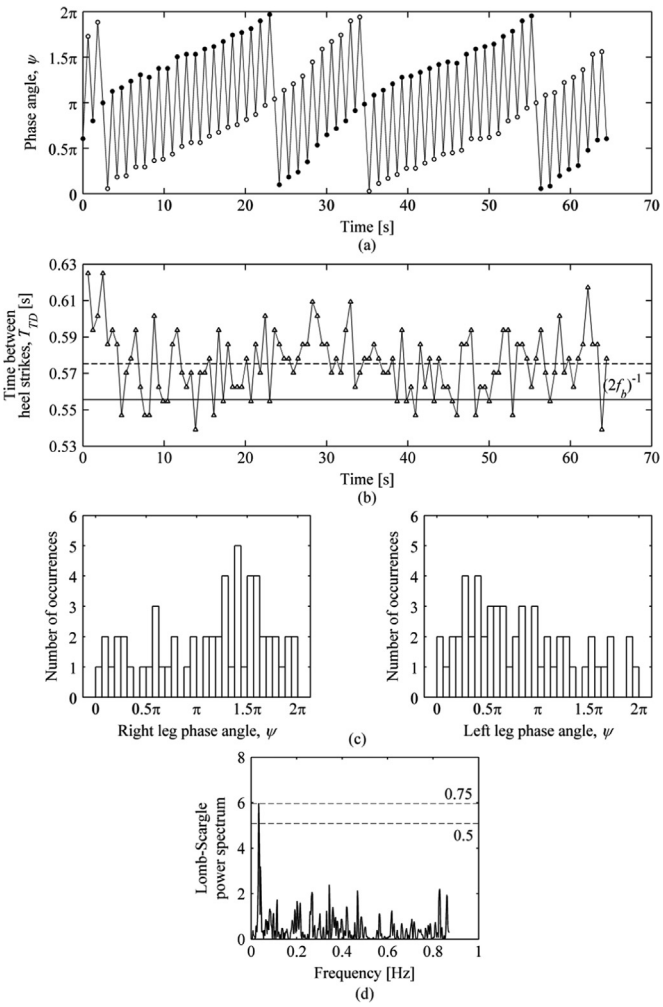

Fig. 5. Pedestrian behaviour and its consequences in the case of phase pulling identified for $f_b = 0.9$Hz, $A = 5$mm, $f_p = 0.87$Hz. (a) Phase angle for right (•) and left (○) leg touchdowns. (b) Time between heel strikes with dashed line representing the mean value and continuous line representing half of the treadmill vibration period. (c) Histograms of phase angles for leg touchdowns with bin size of $\pi/16$. (d) Lomb-Scargle normalised power spectrum of time between heel strikes with significance levels denoted by dashed lines.

between the components of pedestrian-structure system. To this end Fig. 6 presents work done on the bridge by a pedestrian during each step taken between two consecutive contralateral (i.e. opposite) leg touchdowns, obtained from:

$$W_n = \int_{t_{TD,n}}^{t_{TD,n+1}} F_L \dot{x}_b dt \tag{4}$$

where W is the work done on the bridge, n is the step number and F_L is the pedestrian force. F_L was taken as the difference between the measured lateral force during the considered test (i.e. in the presence of a pedestrian) and the force from an empty treadmill oscillating in the same prescribed motion as during that test. It was then filtered with a two-way fourth-order Butterworth low-pass filter with cut-off frequency 6 Hz. The steps starting from the right and left leg touchdowns are denoted by • and ○, respectively. All data in Fig. 6 come from the test described in Section 3.2.1 ($f_b = 0.9$Hz, $A = 10$mm and $f_p = 0.94$Hz) and correspond to data in Fig. 4.

Fig. 6(a) presents the time history of W. It can be seen that W evolves in regular patterns of positive and negative regions of values and that the regions of positive values are more pronounced hence the pedestrian, on average, does positive work on the structure. Since $\Delta\widetilde{C}$ and W only differ in the sign and scaling factors, the pedestrian is in this case inducing a net negative self-excited damping force. This observation has been previously made by Barker [21] and Macdonald [6] from the output of their respective models (see Fig. 3 in [21] and Figs. 7 and 8 in [6]), but this is the first time that this asymmetric behaviour is observed in experimental data.

The work done on the oscillating treadmill is re-plotted in Fig. 6(b) against the compatible phase angle corresponding to the instant of touchdown, marking the beginning of the step. The densification of data points in the region of ψ_c from $\pi/8$ to $17\pi/16$, evident in closely spaced lines, dots and circles, reflects phase pulling visible in Fig. 4 (see e.g. histograms in Fig. 4

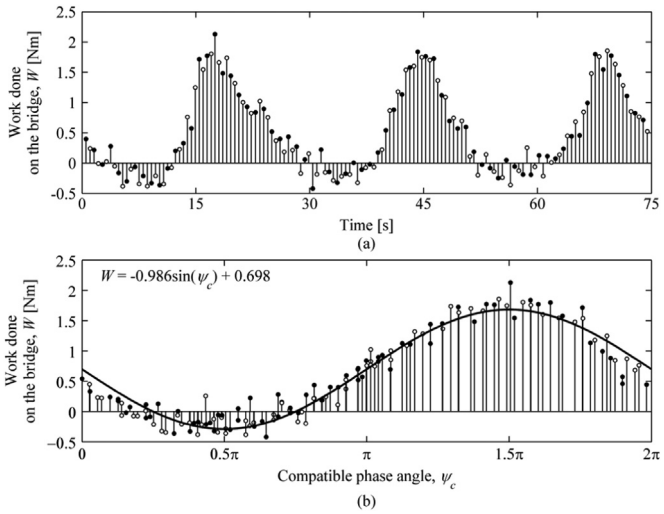

Fig. 6. (a) Time evolution of work done on the oscillating treadmill during steps initiated on touchdowns of the right (•) and left (○) leg. (b) Data from (a) re-plotted against compatible phase angle. Black curve denotes the best sinusoid fitted to these data, described by the equation at the top of the plot.

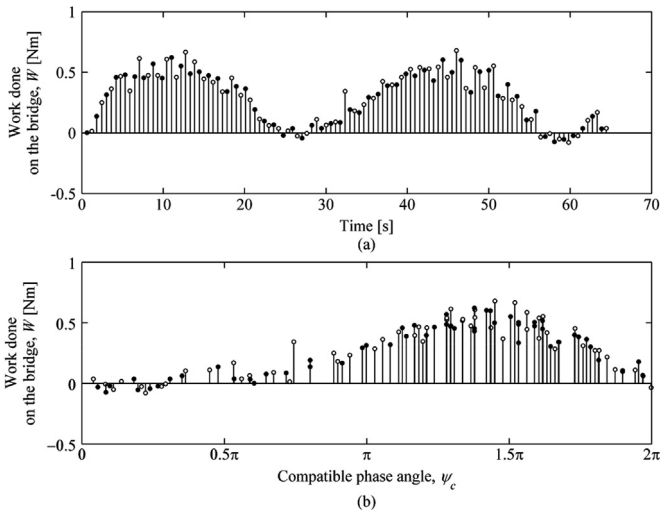

Fig. 7. (a) Time evolution of work done on the oscillating treadmill during steps initiated on touchdowns of the right (•) and left (○) leg. (b) Data from (a) re-plotted against compatible phase angle. Black curve denotes the best sinusoid fitted to these data, described by the equation at the top of the plot.

(c)). It can be seen that the distribution of data points follows a sinusoidal waveform. The best sinusoidal fit to the data is denoted in Fig. 6(b) by a black curve and its equation is given at the top of the plot. The standard error of the fit is 0.18 N m and the adjusted R-square is 0.93, indicating that the fit describes the data reasonably well. Apart from the asymmetry of W visible in Fig. 6(a) discussed earlier, it can be seen that the range of ψ_c for which W is predominantly positive, i.e. from 0 to 0.16π and from 0.76π to 2π, is much wider than the range of ψ_c for which W is predominantly negative, i.e. from 0.16π to 0.76π. Furthermore, the data points are not evenly distributed through the range of ψ_c, but densify around $\pi/2$, which agrees with data in Fig. 4.

The data presented in Fig. 6 reveal the reason for different influence of the bias in the distribution of ψ_c on dynamic structural stability. For example, the bias in the distribution of ψ_c for the two sets of data in Table 3 for which $f_p > f_b$ is similar, with ψ_c most often taking values in the lower half of its whole range. The timing of footsteps for the most populated bins of ψ_c is such that the pedestrian does net negative work on the bridge throughout a step, hence damps its motion. Higher skewness of ψ_c towards its lower range in the set of data in Table 3 for which $f_p = 0.93$Hz implicates that, although steps initiated at higher ψ_c usually generate more destabilising energy transmitted to the structure than the steps initiated at lower ψ_c generating energy damping structural motion, since there are relatively fewer of them, they do not cause the average effect of pedestrian action to be detrimental. In contrast, the distribution of ψ_c for the set of data for which $f_p = 0.94$Hz (see Figs. 4 and 6) exhibits lower skewness hence the net effect of pedestrian action is such to excite structural vibration mode.

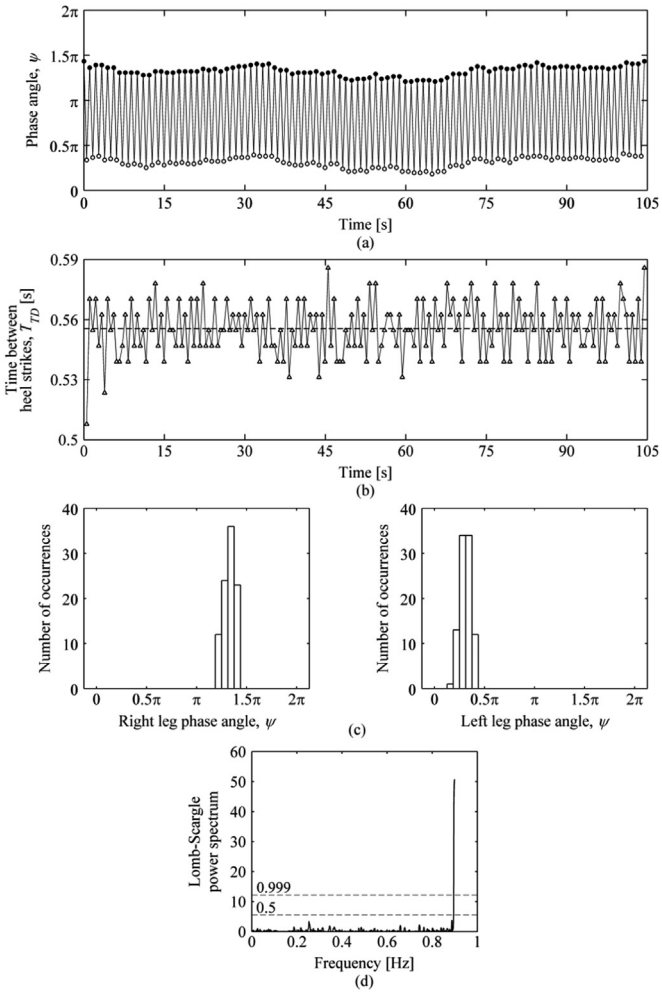

Fig. 8. Pedestrian behaviour and its consequences in the case of frequency entrainment for $f_b = f_p = 0.9$Hz and $A = 10$mm. (a) Phase angle for right (•) and left leg touchdowns (○). (b) Time between heel strikes with dashed line representing the mean value. (c) Histograms of phase angles for leg touchdowns with bin size of $\pi/16$. (d) Lomb-Scargle normalised power spectrum of time between heel strikes with significance levels denoted by dashed lines.

For comparison, a set of plots for work done on the bridge by a pedestrian during each step for the test described in Section 3.2.2 ($f_b = 0.9$Hz, $A = 5$mm and $f_p = 0.87$Hz) is presented in Fig. 7, which corresponds to data in Fig. 5. As in Fig. 6(a), W in Fig. 7(a) evolves in regular patterns of positive and negative regions of values and the regions of positive values are more pronounced hence the pedestrian, on average, does positive work on the structure. The bias in the distribution of ψ_c for the set of data presented in Fig. 5, for which $f_p < f_b$, differs from the results for $f_p > f_b$ presented in Fig. 4 in the preferred ψ_c, which most often falls into the higher half range as can be seen in Fig. 7(b). Consequently, work done on the bridge during most of the steps is positive and $\Delta\widetilde{C}$ is strongly detrimental (see Table 3). Generally lower magnitudes of W and its slightly different envelope (not shown in Fig. 7(b) explicitly due to relatively high variability in pedestrian behaviour) reflect changes in pedestrian-structure interaction pertaining to the treadmill vibration and pedestrian parameters.

3.2.4. Possibility of occurrence of phase pulling

Phase pulling occurred for cases when the average pedestrian stride frequency was within 0.05 Hz (6%) of the lateral vibration frequency, but the maximum magnitude of the difference between the treadmill oscillation and pedestrian stride frequencies reached 0.1 Hz (11%). This suggests phase pulling could be relatively common where the structural frequency falls within the range of typical stride frequencies.

Phase pulling was not observed in the tests with the treadmill oscillating with a lateral displacement amplitude of 15 mm, which was the highest amplitude applied in the tests. However, since only six tests were conducted in these conditions and the criteria adopted in the identification of phase pulling are quite stringent, the possibility of occurrence of this mechanism for displacement amplitudes higher than 10 mm (see Table 3) cannot be discounted.

It is well known that the average walking speed of pedestrians in a crowd reduces with increasing crowd density [22], and that the walking speed has a positive correlation with the walking frequency [23,24]. Therefore, given the effect of the

phase pulling behaviour above, a sudden increase in structural vibration amplitudes could occur when the velocity of a crowd reduces thus causing a decrease in pedestrians' stride frequencies to below the frequency of the excited structural mode. Interestingly, this effect could explain why the pedestrians on the widely publicised video footage of the opening day on the London Millennium Footbridge, during a period of instability, appeared to alternately fall in and out of synchrony with the lateral bridge motion [25]. Furthermore, the outputs from the IPM, derived based on an assumption of invariance of stride frequency, suggest that the magnitudes of ΔC and ΔM are larger for lower stride frequencies (hence walking speeds), causing a more detrimental negative damping effect [7]. Therefore it can be expected that the walking speed of pedestrians in a crowd can be an important factor in determining the dynamic structural stability [12].

The discovered phase pulling mechanism is remarkably similar to the behaviour of the IPM previously used to model pedestrian actions on vertically oscillating structures [26,27]. Unsynchronised and synchronised pedestrian motion was shown to be separated by *intermittency* occurring when the pedestrian stride frequency and the frequency of the excited mode are relatively close. In this dynamic regime the speed of evolution of the instantaneous phase angle changes cyclically in different phase angle ranges (see Fig. 6 in [27]), as the pacing frequency alternately gets closer to the structural vibration frequency and drifts further apart from it in prolonged periods. This is in line with phase pulling presented in Section 3.2.

It was speculated by McRobie et al. [14] that similar behaviour, albeit unimodal – meaning there is only one phase pulling pattern, could occur for walking on a laterally oscillating structure. The subsequent preferential phase frequency entrainment triggered by increasing vibration amplitudes could bias the average ΔC towards more detrimental values, in line with those measured on full-scale structures. This hypothesis is further explored in Section 4.

3.3. Persistent frequency locking (synchronisation)

If persistent frequency locking occurs the phase angles for each leg are expected to be almost constant values. Only two cases in which frequency locking was a dominant stepping behaviour throughout the test were identified in the experimental data, although a few cases of intermittent frequency locking were also identified and are discussed in Section 3.4. These two cases in which $f_p/f_b = 1$ and $f_p/f_b = 2$, respectively, are presented in Sections 3.3.1 and 3.3.2.

3.3.1. Frequency locking for $f_p/f_b = 1$ (frequency entrainment)

The evolution of the phase angle for the case of frequency entrainment is presented in Fig. 8(a). The time history of time between heel strikes is presented in Fig. 8(b) with a mean value of 0.556 s, corresponding to half the treadmill vibration period at $(2f_b)^{-1}$, denoted by a dashed line. It can be seen that the values of time between heel strikes are spaced closely around the mean.

Fig. 8(c) presents the distribution of phase angles. It can be seen that the phase angles are concentrated in narrow bands of $19\pi/16$ to $23\pi/16$ for the right leg and $2\pi/16$ to $7\pi/16$ for the left leg touchdowns, respectively.

Only one dominant component at a frequency of 0.9 Hz, having significance level higher than 0.999, was identified in the normalised power spectrum presented in Fig. 8(d). This indicates that there is a pattern of variation of heel strike intervals with a frequency of 0.9 Hz, i.e. once per full gait cycle, so there is some asymmetry of the gait, but there is no other significant component of the power spectrum.

For the set of data presented in Fig. 8 the pedestrian did work on the moving structure. The right leg touchdowns occurred just before the treadmill started moving to the right and the left leg touchdowns occurred just before the treadmill started moving to the left (see Fig. 2), so the pedestrian force throughout each step was mostly applied in phase with the treadmill velocity. As a result, the equivalent added damping for this case, identified as –1008 Ns/m, is strongly detrimental for structural stability, while the equivalent added mass is negligible.

3.3.2. Frequency locking for $f_p/f_b = 2$

Another example of frequency locking is presented in Fig. 9, for a treadmill amplitude of 10 mm and frequency of 0.54 Hz. It can be seen in Fig. 9(a) that the phase angles for right and left leg touchdowns take values in two distinct ranges separated by π. This means that the subject's stride frequency was twice the treadmill vibration frequency. The time history of the time between heel strikes is presented in Fig. 9(b) with the mean value of 0.462 s, corresponding to a quarter of the treadmill vibration period, denoted by a dashed line.

Fig. 9(c) presents the distribution of phase angles. It can be seen that the phase angles are concentrated in two narrow bands of 0 to $3\pi/16$ and π to $19\pi/16$ for the right leg, and $8\pi/16$ to $11\pi/16$ and $24\pi/16$ to $27\pi/16$ for the left leg touchdowns, respectively. There is only one dominant component at a frequency of 0.54 Hz, with a significance level higher than 0.99, in the Lomb-Scargle normalised power spectrum presented in Fig. 9(d). This means that there is a pattern of variation of heel strike intervals which occurs at the treadmill lateral oscillation frequency.

3.4. Intermittent frequency entrainment

This type of behaviour occurs when the evolution of phase angle is irregular, meaning that the rate of change of phase angle changes in prolonged periods, and the pedestrian stride frequency exhibits intermittent frequency entrainment.

An example case of intermittent frequency entrainment is presented in Fig. 10 for $f_b = 0.9$Hz and $A = 10$mm. Frequency entrainment can be seen in Fig. 10(a) for the regions where phase angle for the right leg takes values close to 0.29π and

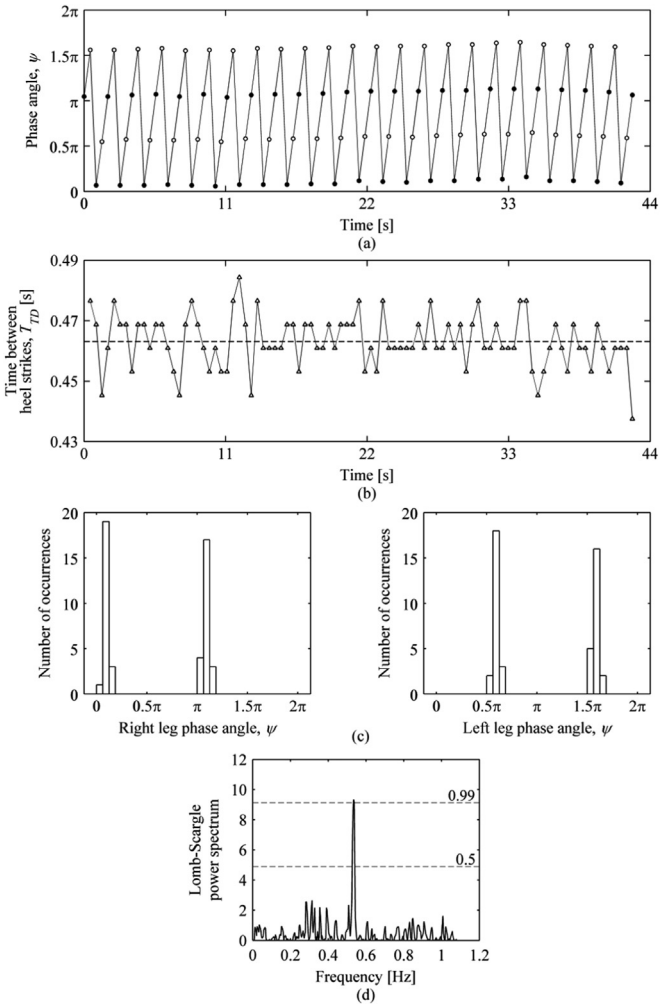

Fig. 9. Pedestrian behaviour and its consequences in case of frequency locking for $f_b = 0.54$Hz, $A = 10$mm and $f_p = 1.08$Hz. (a) Phase angle for right (•) and left (○) leg touchdowns. (b) Time between heel strikes with dashed line representing the mean value. (c) Histograms of phase angles for leg touchdowns with bin size of $\pi/16$. (d) Lomb-Scargle normalised power spectrum of time between heel strikes with significance levels denoted by dashed lines.

0.99π. These regions are separated by periods during which the average (over several steps) rate of change of phase angle deviates significantly from zero. The highest positive and the lowest negative gradients of the evolution of phase angle correspond to the periods in which the pedestrian walked with the lowest and highest stride frequency, respectively, falling below and above the treadmill lateral vibration frequency (cf. Fig. 5 and Fig. 4, respectively). This can be seen in Fig. 10(b) by tracking changes in time between heel strikes. The distributions of phase angle on histograms in Fig. 10(c) show irregular patterns, with the most populated bins corresponding to the entrained phase angles for both legs. However, unlike in Figs. 8 (c) and 9(c), phase angles are not confined to few, but spread to relatively many neighbouring bins. Fig. 10(d) shows several statistically significant components of variability of data in Fig. 10(c), at frequencies of 0.008, 0.877, 0.885 and 0.9 Hz, which reflect changes in pedestrian temporal stepping behaviour throughout the test.

3.5. Non-uniform distribution of phase angles

Non-uniform distribution of phase angles is characterised by randomness in the collected data, in particular lack of evidence of consistency of gait parameters and any type of phase attraction. The phase angle evolves in these cases similarly to the one presented in Fig. 10, however, no intermittent phase locking periods are present.

4. The effect of frequency locking on structural stability

Preferential phase frequency entrainment whereby a pedestrian synchronises their frequency to the frequency of a

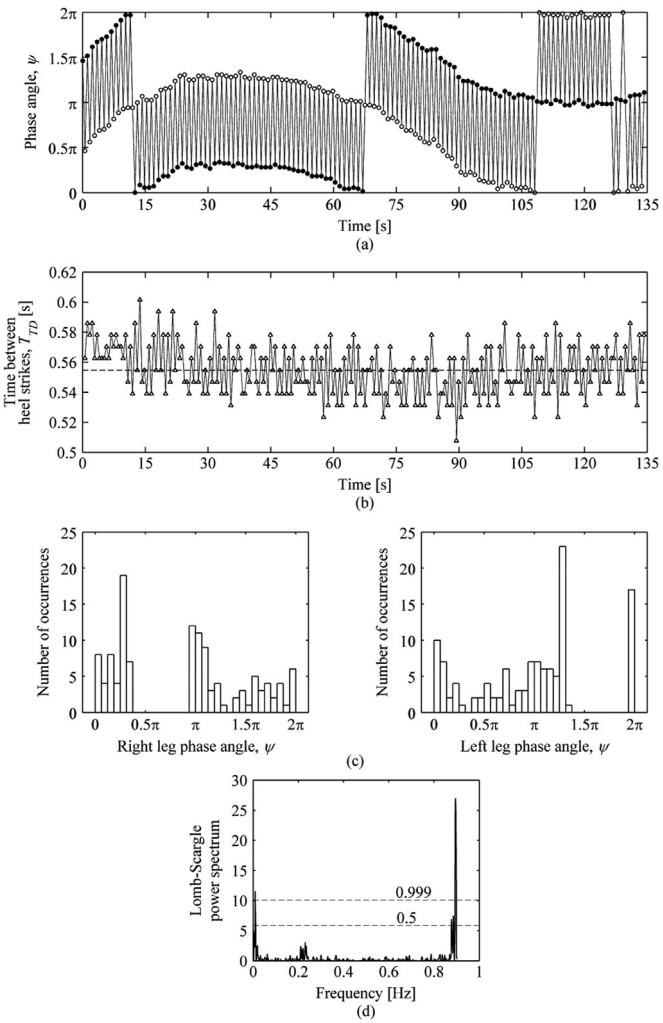

Fig. 10. Pedestrian behaviour and its consequences in the case of intermittent frequency entrainment for $f_b = 0.9$Hz and $A = 10$mm. (a) Phase angle plot for right (•) and left (○) leg touchdowns. (b) Time between heel strikes with dashed line representing the mean value. (c) Histograms of phase angles for leg touchdowns with bin size of $\pi/16$. (d) Lomb-Scargle normalised power spectrum of time between heel strikes with significance levels denoted by dashed lines.

moving structure, adjusting their phase such as to increase structural motion, has been postulated as an explanation for discrepancy in ΔC estimated from the bottom-up and top-down approach (see Section 1). The applicability of this assumption is explored in this section based on experimental data. The experimental results are also related to the predictions of the IPM, which is currently the most promising template of pedestrian behaviour on laterally oscillating structures.

Frequency locking was identified for 6 subjects, in 9 out of 137 tests. The details of these tests, hereafter referred to as T1 to T9, are given in Table 4. During some of the tests the frequency entrainment was intermittent (see Section 3.4) and the subject entrained more than once, but never at the same phase. Therefore Table 4 includes 13 records from all frequency locking periods, a necessary condition for inclusion being that the period lasted for at least 10 s and the variability of phase angle quantified in terms of standard deviation had to be within $\pm 0.05\pi$. This prevented spurious identification of synchronisation at the same time allowing for the possibility of intermittency in this behaviour. For completeness, Table 4 also includes the results from the test during which a subject walked with the stride frequency equal twice the treadmill lateral oscillation frequency (T3), discussed in Section 3.3 and presented in more detail in Fig. 9.

Frequency entrainment occurred most often during tests conducted at the vibration amplitude and frequency of 10 mm and 0.9 Hz, respectively. These are also the vibratory conditions applied in the most number of tests (44 out of 137). Considering all the data in Table 4, the average body-mass normalised equivalent added damping and mass were, respectively, $-3.32\ \mathrm{s}^{-1}$ and -0.49. Converting these values to units allowing comparison with data in Table 1 while accounting for the population statistics in Table 4, by taking the weighted means with relation to the pedestrian mass and the duration of frequency entrainment period, these correspond to -415 N s m^{-1} and -42 kg for and ΔM, respectively. Therefore, on average, based on the data in Table 4, synchronisation had a relatively strong negative added damping effect

Table 4
Body weight normalised equivalent added damping and mass for all tests in which synchronisation of pedestrian footsteps to the lateral treadmill oscillation was identified. Entrained compatible phase is the upper boundary of the most populated bin within a histogram of a compatible phase angle having a bin size of $\pi/16$.

Test ID	Gender	Height h [m]	Mass m_p [kg]	Vibration amplitude A [mm]	Vibration frequency f_b [Hz]	Entrained compatible phase ψ_c [$\times\pi/16$; rad]	Normalised equivalent added damping $\Delta C/m_p$ [s^{-1}]	Normalised equivalent added mass $\Delta M/m_p$ [n/a]
T1	male	1.76	78	5	0.9	30	−4.99	2.36
T2	male	1.87	104	5	0.9	2	8.48	1.69
T3[b,a]	male	1.86	92	10	0.54	18 & 2	−2.47	−2.07
T4	male†	1.81	75	10	0.9	16	−5.51	−2.07
T4	male†	1.81	75	10	0.9	13	4.71	−1.88
T5	male†	1.81	75	10	0.9	16	−6.59	−2.17
T6[a]	male‡	1.99	87	10	0.9	22	−11.61	−0.02
T7	male‡	1.99	87	10	0.9	2	0.26	0.79
T7	male‡	1.99	87	10	0.9	19	−8.84	−0.74
T8	male‡	1.99	87	10	0.9	5	1.55	0.37
T8	male‡	1.99	87	10	0.9	16	−5.74	−0.92
T9	male‡†	1.84	85	15	0.9	13	1.75	−1.46
T9	male‡†	1.84	85	15	0.9	18	−6.18	−1.61

†, ‡ and ‡† denote the 3 subjects for which phase entrainment was identified in more than one test or at multiple phases.
[a] denotes tests during which synchronisation was the dominant stepping behaviour (see Section 3.3).
[b] denotes the test during which the subject's stride frequency was twice the treadmill lateral oscillation frequency (see Section 3.3.2).

detrimental and, contrary to what might be expected, pedestrians would effectively reduce the modal mass of the vibrating mode. This may give some support to the preferential phase entrainment notion suggested by McRobie [14]. However, in the derivation of this average value, ΔC from Table 4 were reweighted by the duration of the frequency entrainment periods and hence were strongly biased towards the result from a single test in which frequency entrainment was the dominant pedestrian stepping behaviour and ΔC was overall the most detrimental.

It may be speculated that phase pulling is an intermediate step towards frequency entrainment. However, no definite phase preference during the synchronisation periods can be seen in the data presented in Section 4, which would be then expected. The results reported in [5] seem to concur in this respect. This might suggest that the test subjects synchronised with the treadmill oscillation at the identified phases by chance rather than due to a synchronisation transition [16]. Therefore, it is believed that synchronisation is not the main mechanism causing the discrepancy between the self-excited forces derived using bottom-up and top-down approaches (see Section 1).

To be able to relate the current results to the predictions of the IPM, analytical formulations of the quasi self-excited forces for the case of frequency entrainment are first presented in a form allowing direct comparison and some relevant issues related to the performance of the IPM are discussed in the next section.

4.1. Analytical formulation of the quasi self-excited forces for frequency entrainment

Analytical expressions describing the phase-dependent magnitudes of the quasi self-excited forces for the IPM [6] in the case of frequency entrainment were derived by McRobie [28]. Converting these expressions to account for the phase angle convention adopted herein (see Section 2.4), these are:

$$\Delta C(\omega_b) = -\frac{2m_p\Omega_p^2\left(1+e^{\frac{\Omega_p}{2f_p}}\right)}{\pi^2\omega_b\left[1+\left(\frac{\Omega_p}{\omega_b}\right)^2\right]^2}\sin\ \psi_c\gamma \tag{5}$$

$$\Delta M(\omega_b) = \frac{2m_p\Omega_p^2}{\omega_b^2\left[1+\left(\frac{\Omega_p}{\omega_b}\right)^2\right]}\left\{\frac{1}{2}-\frac{1+e^{\frac{\Omega_p}{2f_p}}}{\pi\left[1+\left(\frac{\Omega_p}{\omega_b}\right)^2\right]}\cos\ \psi_c\gamma\right\} \tag{6}$$

where

$$\gamma = \left\{1-\kappa_0\left[1+\left(\frac{\Omega_p}{\omega_b}\right)^2\right]\right\}\sin\ \psi_c + \frac{\omega_b}{\Omega_p}\left\{1-\kappa_1\left[1-\left(\frac{\Omega_p}{\omega_b}\right)^2\right]\right\}\cos\ \psi_c - \frac{b_{\min}}{A}\left[1+\left(\frac{\Omega_p}{\omega_b}\right)^2\right] \tag{7}$$

In the above expressions m_p is the pedestrian mass, $\Omega_p = \sqrt{g/l}$ is the angular frequency of the IPM with g and l denoting

gravitational acceleration and pendulum leg length, respectively, and $b_{\min}$ is the constant defined by Hof et al. [29] as the margin of stability. The coefficients κ_0 and κ_1 allow, within the solution of the IPM, for different variants of the foot placement control law to be readily considered:

$$u = x_{\mathrm{CoM}} + \kappa_0 x_b + \frac{\dot{x}_{\mathrm{CoM}}}{\Omega_p} + \kappa_1 \frac{\dot{x}_b}{\Omega_p} \pm b_{\min} \tag{8}$$

where u is the lateral position of the foot at the instant of heel strike (taken at a point), x_{CoM} is the lateral position of the centre of mass (CoM), x_b is the lateral position of the bridge and dots over symbols denote differentiation with respect to time. According to Eq. (8), the pedestrian will place their foot laterally (i.e. in the frontal plane) at a position dependent on the lateral velocity of the CoM at the instant of heel strike, offset by $b_{\min}$. In the original formulation of the IPM [6] two versions of Eq. (8) were presented, since the velocity of CoM could be taken relative to the bridge, or to an absolute reference point. To account for these two scenarios, κ_0 and κ_1 take values $[\kappa_0, \kappa_1] = [0, 0]$ for the relative velocity control law, when $\dot{x}_{\mathrm{CoM}}$ is taken relative to the bridge ($\dot{x}^{\mathrm{rel}}_{\mathrm{CoM}}$), and $[\kappa_0, \kappa_1] = [0, 1]$ for the absolute velocity control law, when $\dot{x}_{\mathrm{CoM}}$ is taken relative to a stationary point outside the bridge ($\dot{x}^{\mathrm{abs}}_{\mathrm{CoM}}$).

It is worth noting that Eqs. (5) and (6) show dependence of the self-excited forces on $b_{\min}$ and A via Eq. (7), which is not the case for the IPM for phase drift. In that case the long-term average pedestrian force is equal to the sum of the pedestrian force for walking on stationary ground and the self-excited forces. The former is proportional to $b_{\min}$ but the latter are independent of it. For the case of phase entrainment the force for walking on stationary ground and the dominant self-excited force act at the same frequency, so they cannot be distinguished from each other in empirical measurements. To be compatible with this, Eqs. (5) and (6) treat them together, so hence give amplitude dependent equivalent added damping and mass. However, since according to the analysis, part of the forcing is not actually self-excited, the forces from Eqs. (5) and (6) will be hereafter termed quasi self-excited forces.

4.2. Comparison of the predictions of the IPM with experimental data

Additional steps in data processing are necessary for the experimental results to be compatible with the outputs of the IPM described in Section 4.1 thus allowing direct comparison. Human walking gait comprises of single and double support phases in which one and both feet are in contact with the walking surface, respectively. For simplicity, the IPM does not model the double support stance phase and the transition between steps is taken as instantaneous, occurring at the mid double support. Clearly, this instant does not correspond to the instant of foot placement identified from the experimental data which marks the beginning of the double support phase of gait and was used to obtain ψ_c. Therefore, the identified phase angle was offset by half the average duration of the double support period, normalised by the bridge vibration period and converted to an angular scale.

The following sections present the results of comparison of the predictions of the IPM with experimental data. The comparison is split into two parts addressing amplitude and phase dependence of the quasi self-excited forces, respectively. Since the pedestrian mass, m_p, scales ΔC and ΔM directly, the quasi self-excited forces are presented normalised by that parameter ($\Delta\widetilde{C}$ and $\Delta\widetilde{M}$). The amplitude dependence of $\Delta\widetilde{C}$ and $\Delta\widetilde{M}$ is shown based on results from T1, T2, T4, T5 and T9. This is to account for the influence of the leg length (via the term $\Omega_p = \sqrt{g/l}$ in Eqs. (5) and (6)) which is correlated to the pedestrian height, since T6, T7 and T8 were conducted with a pedestrian much taller than the rest of the group (see Table 4). Furthermore, since the most complete set of results obtained for a single pedestrian for the same treadmill vibratory conditions was assembled for the latter set of tests, that set is used to show the phase dependence of $\Delta\widetilde{C}$ and $\Delta\widetilde{M}$. For the same reason only the results from that latter set of tests are used in quantification of the predictive power of the IPM. T3 is not further considered since this was the only test during which the pedestrian locked their stride frequency to the frequency of the lateral treadmill motion with a 2:1 ratio.

4.2.1. Amplitude dependence of the quasi self-excited forces in the case of frequency entrainment

The following values of parameters were used to obtain the quasi self-excited forces from Eqs. (5) and (6): $f_b = f_p = 0.9$Hz, $b_{\min} = 15.7$mm, $A = \{5, 10, 15\}$mm and, as in Hof et al. [30], $l = 1.34 l_{\mathrm{leg}}$. The representative value of the leg length, l_{leg}, had to be chosen based on the population statistics from T1, T2, T4, T5 and T9 (see Table 4). The relationship between height and leg length, established (although not given explicitly) for male subjects by Pheasant [31] was used:

$$l_{\mathrm{leg}} = 0.7028h - 0.3091 \tag{9}$$

where h is the height in metres taken from Table 4, to find the weighted mean l_{leg} over all subjects from the relevant population (=0.97m). The amplitude dependence of $\Delta\widetilde{C}$ and $\Delta\widetilde{M}$ in the case of frequency entrainment, for the experimental results and from the IPM Eqs. (5) and (6), based on both relative and absolute velocity foot placement control laws, is shown in Fig. 11.

It can be seen in Fig. 11 that the experimental points generally agree with the output from the IPM in sign. A very good match for both $\Delta\widetilde{C}$ and $\Delta\widetilde{M}$ can be seen for T1 and T2, for which the vibration amplitude was 5 mm, for the foot placement control law based on $\dot{x}^{\mathrm{abs}}_{\mathrm{CoM}}$. A reasonable match for both $\Delta\widetilde{C}$ and $\Delta\widetilde{M}$ can also be seen for T9, for which the vibration amplitude was 15 mm, although the foot placement control law based on $\dot{x}^{\mathrm{rel}}_{\mathrm{CoM}}$ seems more applicable in this case.

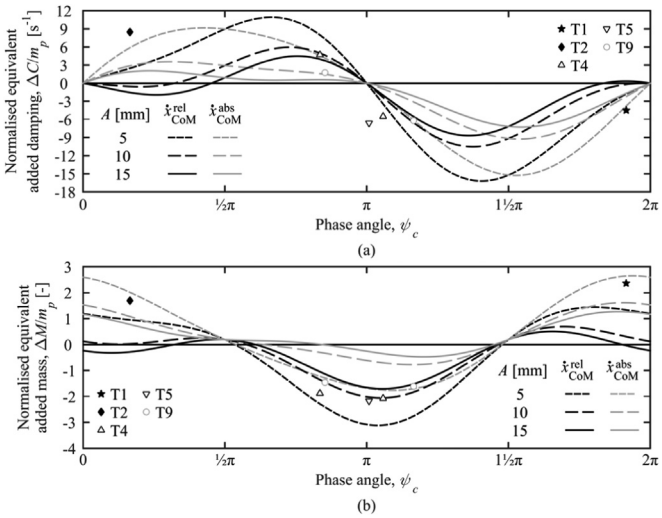

Fig. 11. (a) Normalised equivalent added damping and (b) normalised equivalent added mass for synchronisation periods during tests T1, T2, T4, T5 and T9. Black and grey curves represent the results from the IPM based on relative and absolute velocity foot placement control law, respectively.

Experimental data from T4 and T5, for which the vibration amplitude was 10 mm, seem to match the results from the IPM for $\Delta\widetilde{M}$ derived with the foot placement control law based on $\dot{x}^{rel}_{CoM}$. This is also true for $\Delta\widetilde{C}$ obtained during T4 at the lower ψ_c, however, less agreement can be seen for $\Delta\widetilde{C}$ obtained for T4 at the higher ψ_c and for T5, for which the experimental data are shifted towards lower ψ_c relative to values from the IPM. It is noteworthy that these data points are near the zero crossing, where the rate of change of the function in Eq. (5) is relatively high, hence small lateral shifts in ψ_c cause large discrepancies between the results.

4.2.2. Phase dependence of the quasi self-excited forces in the case of frequency entrainment

The following values of parameters were used to obtain the quasi self-excited forces from Eqs. (5) and (6): $f_b = f_p = 0.9$Hz, $b_{min} = 15.7$mm, $A = 10$mm and $l = 1.46$m. The phase dependence of $\Delta\widetilde{C}$ and $\Delta\widetilde{M}$ in the case of phase entrainment, for the experimental results from T6, T7 and T8 (see Table 4) and data from the IPM, based on both relative and absolute velocity foot placement control laws, is shown in Fig. 12.

It can be seen in Fig. 12 that the foot placement control law based on $\dot{x}^{rel}_{CoM}$ gives a better match with the experimental results in the case of $\Delta\widetilde{C}$, although $\Delta\widetilde{C}$ for T6 falls well below the model prediction. However, a better match for $\Delta\widetilde{M}$ can be seen for the output of the IPM based on $\dot{x}^{abs}_{CoM}$. The normalised root-mean-square errors, calculated by dividing root-mean-square error by the mean of five experimental observations, are -32% and -69% for $\Delta\widetilde{C}$, and 30% and 10% for $\Delta\widetilde{M}$, for the output of IPM based on $\dot{x}^{rel}_{CoM}$ and $\dot{x}^{abs}_{CoM}$, respectively. These quantitative results, analogous to the coefficients of variation,

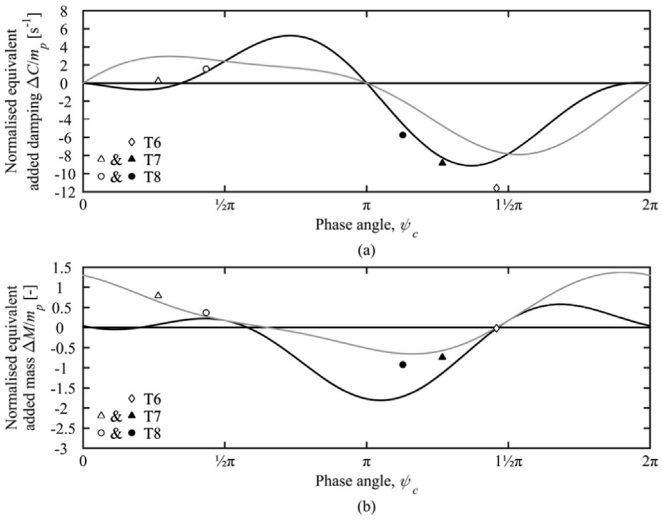

Fig. 12. (a) Normalised equivalent added damping and (b) normalised equivalent added mass for synchronisation periods during tests T6, T7 and T8. Black and grey curves represent the results from the IPM based on relative and absolute velocity foot placement control law, respectively.

should be taken with care since the limited number of experimental data does not guarantee strong statistical power. Considering all data in Fig. 12, it can be concluded that the test subject, on average, synchronised their gait to the treadmill motion such as to input energy into the vibrating mode.

4.3. Applicability of the inverted pendulum pedestrian model

The results presented in Section 4.2 suggest that the IPM performs well in explaining the trend in quasi self-excited forces in the case of frequency entrainment. Although there is some scatter of experimental data around the simulated results, some of it can be associated with variability in pedestrian gait throughout a test. An issue which still needs to be addressed is the form of the foot placement control law which should be used within the IPM and this requires further investigations [32], and indeed other refinements of the model could be considered. Nevertheless, it can be concluded that the IPM is a good template for pedestrian behaviour on laterally oscillating structures. It is the only model currently available which has been shown to be able to explain all the components of pedestrian lateral loading on laterally oscillating structures in the presence of single- [11] and multi-modal [33] structural motion. Furthermore, the low-dimensionality of the model means it easily lends itself to modifications allowing the phase pulling mechanism to be incorporated [14].

5. Conclusions

A variety of pedestrian stepping behaviour on laterally oscillating structures has been identified experimentally in this study. Phase drift, in which the pedestrian stride frequency differs from the frequency of structural motion so the relative phase evolves at a nearly constant rate, is the most common behaviour. This supports the assumptions made in the use of the inverted pendulum pedestrian model [6,7,12]. However, the evidence has been found for adaptive timing of pedestrian footsteps, classified in this study as phase pulling. This behaviour, identified here for the first time in experimental data, reveals itself in a pattern of evolution of phase between the pedestrian and structural motion in which the rate of change of phase changes systematically in well-defined phase ranges. This observed weak form of modulation of the timing of footsteps can cause the magnitudes of the self-excited forces to be significantly changed in comparison to the case of phase drift.

The discovered phase pulling mechanism can apparently cause a different bias in the timing of footsteps, depending on whether the stride frequency falls below or above the lateral oscillation frequency. This is similar to predictions of the inverted pendulum pedestrian model previously studied in the context of walking on vertically oscillating structures [26,27]. The most detrimental effect for structural stability is when the stride frequency falls below the frequency of the structural mode. The equivalent added damping can then fall well below the values obtained from measurements on full scale bridges, reaching approximately -9 N s m^{-1} s/m per kilogram of pedestrian mass. This is particularly pronounced for relatively slow walking speeds, indicating that structural instability could develop quickly when the speed of pedestrians reduces, e.g. as can be expected with the densification of a crowd, such that their stride frequencies fall below the frequency of the structural mode.

Evidence for persistent and intermittent frequency locking has also been found, although this behaviour was relatively rare. The lack of consistency of the entrained phase between the pedestrian and the bridge motion in these cases suggests that pedestrians might not have a well-defined preferred synchronisation mode, at least in the experimental regime tested.

Comparison of the experimental data and outputs from the inverted pendulum pedestrian model in the case of frequency entrainment has revealed that the model can capture the dependence of (quasi) self-excited forces on the amplitude of motion and the entrained phase. However, further investigation is necessary to determine the foot placement control law applicable for walking on laterally oscillating ground and thus calibrate the model.

The findings from this study support the argument that the tendency of pedestrians to synchronise with lateral structural motion is weak, at least for the vibration conditions applied in the tests, and that synchronisation is not the main mechanism leading to dynamic instability. Instead, it is phase pulling that may explain the under-estimation of negative damping coefficients in models and results from treadmill tests in comparison with previously reported site measurements.

Acknowledgements

Mateusz Bocian was supported by the UK Engineering and Physical Sciences Research Council via the University of Bristol Doctoral Training Account (EP/P50483X) for a part of the work presented in this study. The Wellcome Trust (089367/Z/09/Z) is acknowledged for funding for the experimental setup, through an infrastructure development grant to the Bristol Vision Institute. Professor Alan R. Champneys of the Department of Engineering Mathematics at the University of Bristol is acknowledged for providing comments leading to the improvement of the manuscript.

References

[1] E.T. Ingólfsson, C.T. Georgakis, J. Jönsson, Pedestrian-induced lateral vibrations of footbridges: a literature review, *Eng. Struct.* 45 (2012) 21–52, http://dx.doi.org/10.1016/j.engstruct.2012.05.038.

[2] P. Dallard, A.J. Fitzpatrick, A. Flint, S. Le Bourva, A. Low, R.M. Ridsdill Smith, M. Willford, The London Millennium Footbridge, *Struct. Eng.* 79 (22) (2001) 17–33.

[3] A.D. Pizzimenti, F. Ricciardelli, Experimental evaluation of the dynamic lateral loading of footbridges by walking pedestrians, in: Proceedings of Eurodyn 2005 - the Sixth International Conference on Structural Dynamics, Paris, France, 2005.

[4] T. Theodorsen, *General Theory of Aerodynamic Instability and the Mechanism of Flutter* (Report number: NACA-TR-496), National Advisory Committee for Aeronautics, Longley Field, USA, 1949.

[5] E.T. Ingólfsson, C.T. Georgakis, F. Ricciardelli, J. Jönsson, Experimental identification of pedestrian-induced lateral forces on footbridges, *J. Sound Vib.* 330 (6) (2011) 1265–1284, http://dx.doi.org/10.1016/j.jsv.2010.09.034.

[6] J.H.G. Macdonald, Lateral excitation of bridges by balancing pedestrians, *Proc. R. Soc. A - Math. Phys. Eng. Sci.* 465 (2009) 1055–1073, http://dx.doi.org/10.1098/rspa.2008.0367.

[7] M. Bocian, J.H.G. Macdonald, J.F. Burn, Biomechanically inspired modelling of pedestrian-induced forces on laterally oscillating structures, *J. Sound Vib.* 331 (16) (2012) 3914–3929, http://dx.doi.org/10.1016/j.jsv.2012.03.023.

[8] J.M.W. Brownjohn, P. Fok, M. Roche, P. Omenzetter, Long span steel pedestrian bridge at Singapore Changi Airport - part 2: crowd loading tests and vibration mitigation measures, *Struct. Eng.* 82 (16) (2004) 28–34.

[9] J.H.G. Macdonald, Pedestrian-induced vibrations of the Clifton Suspension Bridge, UK, *Proc. Inst. Civil. Eng. - Bridge Eng.* 161 (2008) 69–77, http://dx.doi.org/10.1680/bren.2008.161.2.69.

[10] E. Caetano, Á. Cunha, F. Magalhaes, C. Moutinho, Studies for controlling human-induced vibration of the Pedro e Inês footbridge, Portugal. Part 1: assessment of dynamic behaviour, *Eng. Struct.* 32 (4) (2010) 1069–1081, http://dx.doi.org/10.1016/j.engstruct.2009.12.034.

[11] M. Bocian, J.H.G. Macdonald, J.F. Burn, D. Redmill, Experimental identification of the behaviour of and lateral forces from freely-walking pedestrians on laterally oscillating structures in a virtual reality environment, *Eng. Struct.* 105 (2015) 62–75, http://dx.doi.org/10.1016/engstruct.2015.09.043.

[12] M. Bocian, J.H.G. Macdonald, J.F. Burn, Probabilistic criteria for lateral dynamic stability of bridges under crowd loading, *Comput. Struct.* 136 (2014) 108–119, http://dx.doi.org/10.1016/j.compstruc.2014.02.003.

[13] S.H. Strogatz, D.M. Abrams, A. McRobie, B. Eckhardt, E. Ott, Crowd synchrony on the Millennium Bridge, *Nature* 438 (2005) 43–44, http://dx.doi.org/10.1038/438043a.

[14] A. McRobie, G. Morgenthal, D. Abrams, J. Prendergast, Parallels between wind and crowd loading of bridges, *Philos. Trans. R. Soc. A – Math. Phys. Eng. Sci.* 371 (20120430) (2013) http://dx.doi.org/10.1098/rsta.2012.0430.

[15] M. Bocian, *Determination of the Self-excited Forces on Structures Due to Walking Pedestrians Using a Biologically-Inspired Approach (PhD thesis)*, Departent of Civil Engineering and Department of Mechanical Engineering, University of Bristol, Bristol, UK., 2014.

[16] A. Pikovsky, M. Rosenblum, J. Kurths, *Synchronization – a Universal Concept in Nonlinear Science*, Cambridge University Press, Cambridge, UK, 2001.

[17] C.M. O'Connor, S.K. Thorpe, M.J. O'Malley, C.L. Vaughan, Automatic detection of gait events using kinematic data, *Gait Posture* 25 (3) (2007) 469–474, http://dx.doi.org/10.1016/j.gaitpost.2006.05.016.

[18] S. Ghoussayni, C. Stevens, S. Durham, D. Ewins, Assessment and validation of a simple automated method for the detection of gait events and intervals, *Gait Posture* 20 (3) (2004) 266–272, http://dx.doi.org/10.1016/j.gaitpost.2003.10.001.

[19] J.D. Scargle, Studies in astronomical time series analysis. III – Fourier transforms, autocorrelation functions, and cross-correlation functions of unevenly spaced data, *Astrophys. J.* 343 (1989) 874–887, http://dx.doi.org/10.1086/167757.

[20] W.H. Press, S.A. Teukolsky, W.T. Vetterling, B.P. Flannery, *Numerical Recipes in FORTRAN, The Art of Scientific Computing*, 2nd ed, Cambridge University Press, Cambridge, UK, 1992.

[21] C. Barker, Some observations on the nature of the mechanism that drives the self-excited lateral reponse of footbridges, in: Proceedings of Footbridge 2002 - the First International Conference, Paris, France, 2002.

[22] Z. Fang, S.M. Lo, J.A. Lu, On the relationship between crowd density and movement velocity, *Fire Saf. J.* 38 (2003) 271–283, http://dx.doi.org/10.1016/S0379-7112(02)00058-9.

[23] J.E.A. Bertram, A. Ruina, Multiple walking speed-frequency relations are predicted by constraint optimization, *J. Theor. Biol.* 209 (4) (2001) 445–453, http://dx.doi.org/10.1006/jtbi.2001.2279.

[24] H.V. Dang, S. Živanović, Experimental characterisation of walking locomotion on rigid level surfaces using motion capture system, *Eng. Struct.* 91 (2015) 141–154, http://dx.doi.org/10.1016/j.engstruct.2015.03.003.

[25] P. Dallard, A.J. Fitzpatrick, A. Flint, A. Low, R.M. Ridsdill Smith, M. Willford, London Millennium Bridge: pedestrian-induced lateral vibration, *J. Bridge Eng.* 6 (6) (2001) 412–417, http://dx.doi.org/10.1061/(ASCE)1084-0702(2001)6:6(412).

[26] M. Bocian, J.H.G. Macdonald, J.F. Burn, Modelling of self-excited vertical forces on structures due to walking pedestrians, in: Proceedings of Eurodyn 2011 - the Eight International Conference on Structural Dynamics, Leuven, Belgium, 2011.

[27] M. Bocian, J.H.G. Macdonald, J.F. Burn, Biomechanically-inspired modelling of pedestrian-induced vertical self-excited forces, *J. Bridge Eng.* 18 (12) (2013) 1336–1346, http://dx.doi.org/10.1061/(ASCE)BE.1943-5592.0000490.

[28] A. McRobie, Long-term solutions of Macdonald's model for pedestrian-induced lateral forces, *J. Sound Vib.* 332 (11) (2013) 2846–2855, http://dx.doi.org/10.1016/j.jsv.2012.12.027.

[29] A.L. Hof, R.M. van Bockel, T. Schoppen, K. Postema, Control of lateral balance in walking - experimental findings in normal subjects and above-knee amputees, *Gait Posture* 25 (2007) 250–258, http://dx.doi.org/10.1016/j.gaitpost.2006.04.013.

[30] A.L. Hof, M.G.J. Gazendam, W.E. Sinke, The condition for dynamic stability, *J. Biomech.* 38 (2005) 1–8, http://dx.doi.org/10.1016/j.jbiomech.2004.03.025.

[31] S.T. Pheasant, Anthropometric estimates for British civilian adults, *Ergonomics* 25 (1982) 993–1001.

[32] S.P. Carroll, J.S. Owen, M.F.M. Hussein, Experimental identification of the lateral human-structure interaction mechanism and assessment of the inverted-pendulum biomechanical model, *J. Sound Vib.* 333 (22) (2014) 5865–5884, http://dx.doi.org/10.1016/j.jsv.2014.06.022.

[33] M. Bocian, J.H.G. Macdonald, J.F. Burn, Determination of pedestrian loads in the presence of multi-modal lateral bridge vibrations, in: Proceedings of Eurodyn 2014 - the Ninth International Conference on Structural Dynamics, Porto, Portugal, 2014.